ELSEVIER

Spectrochimica Acta Part A 56 (2000) 301–307

SPECTROCHIMICA ACTA PART A

www.elsevier.nl/locate/saa

Spin glass formation in $La_{0.9}Sr_{0.1}CoO_3$ catalyst for flameless combustion of methane

C. Oliva [a,*], L. Forni [a], A.V. Vishniakov [b]

[a] *Dipartimento di Chimica Fisica ed Elettrochimica e CSRSRC of CNR, University of Milan, Milan, Italy*
[b] *D.I. Mendeleev University of Chemical Technology of Russia, Moscow, Russia*

Received 10 June 1999; accepted 17 September 1999

Abstract

Two samples of composition $La_{0.9}M_{0.1}CoO_3$ (M = Sr, Ce) have been compared as catalysts for the flameless combustion of methane. The former showed a lower activity than the latter and this difference was enhanced at lower temperature. Aiming at understanding the origin of this behaviour, EPR analysis was carried out at temperatures down to 100 K. At $T < 245$ K a zero-field intense feature appeared with the M = Sr sample only, characterized by opposite phase with respect to the $g \sim 2$ line. This zero-field line was attributed to microwave absorption by spin glass formed by cobalt- and oxygen-based paramagnetic ions. The tendency to strong interaction among these species could also be a reason of the low oxygen availability for the catalytic methane oxidation at higher temperature.

Keywords: Spin glass; Perovskites; Catalytic flameless methane combustion

1. Introduction

In a previous paper [1] some perovskite-type mixed oxides $La_{1-x}M_xCoO_3$ (M = Ce,Sr) were compared to each other as catalysts for the flameless combustion of methane. In particular, it was found that when $x = 0.1$ the Ce-doped catalyst was more active than the Sr-doped one. Indeed, TPD analysis showed a larger amount of available oxygen with the former than with the latter and than with any other Sr-doped samples. Furthermore, XPS data indicated that the partial substitution of Ce^{4+} for La^{3+} caused the presence of larger amounts of Co^{2+}, acting as active sites for oxygen absorption from gas phase, i.e. for catalyst reoxidation. In a following paper [2] the best catalysts of the above mentioned series, i.e. those with M = Ce and different values of x, have been examined in full detail. However, in neither of the two papers the catalyst with $x = 0.1$ and M = Ce was compared to the one having the same value of x but with M = Sr. In this paper we carried out this comparison, aiming at a better understanding of the catalytic mechanism lying under the higher activity of the samples with M = Ce with respect to those with a different ion substituting for La.

* Corresponding author.
E-mail address: oliv@csrsrc.mi.cnr.it (C. Oliva)

1386-1425/00/$ - see front matter
PII: S1386-1425(99)00240-1

2. Experimental

The $La_{0.9}M_{0.1}CoO_3$ (M = Sr, Ce) samples were prepared [2] by addition of a solution of citric acid and ethylene glycol to a boiling solution of La, Sr (or Ce), Co nitrates, followed by evaporation under vigorous stirring till the formation of the gel, drying on a hot plate, heating at 573 K for 6 h and calcination at 1223 K in flowing air for 30 h. The XRD analysis showed only the perovskite-like crystalline phase. BET surface area was ca. 4.5 $m^2\ g^{-1}$ for both samples. The EPR spectra were recorded by means of a Bruker ESP300 spectrometer at temperatures ranging between 100 and 300 K and both with magnetic field increasing and decreasing in the range between 0 and 8000 G. The profile of the EPR spectrum obtained at room temperature with $La_{0.9}Sr_{0.1}CoO_3$ after catalytic use has been simulated by the Bruker SimFonia programme. The catalytic activity for the flameless combustion of methane was measured by loading 0.2 g of catalyst in a continuous bench microreactor 0.7 mm ID, to which a mixture of 20 $cm^3\ min^{-1}$ of 1 vol% CH_4 in N_2 and 20 $cm^3\ min^{-1}$ air was fed, while increasing temperature by 2 K min^{-1} from 550 up to 873 K.

Table 1

Parameter	$La_{0.9}Ce_{0.1}CoO_3$	$La_{0.9}Sr_{0.1}CoO_3$
$T_{1/2}$ (K)[a]	807	803
Specific activity at $T_{1/2}$[b]	45.0×10^{-3}	52.0×10^{-3}
Specific activity at 623 K[b]	3.00×10^{-3}	0.25×10^{-3}
Specific activity at 823 K[b]	52.00×10^{-3}	47.00×10^{-3}
Specific activity at 873 K[b,c]	75.0×10^{-3}	65.0×10^{-3}
CH_4 mol% convers. at 623 K	3.5	1
CH_4 mol% convers. at 823 K	60	62

[a] Temperature at which 50% of methane conversion is obtained.

[b] In mol conv./m^2 min.

[c] Temperature of highest methane conversion.

3. Results

3.1. Catalytic activity

The specific activity of the two samples is compared in Fig. 1. In Table 1 a few performance parameters characterizing the two catalysts are reported. It is worth to observe that while some of them are rather similar for the two samples, other are not. In particular, the temperature $T_{1/2}$ (50% methane conversion), as well as the specific activity and the conversion at temperatures higher than $T_{1/2}$ are not too different. In any case the best catalyst is the one with M = Ce, the only parameter a bit unfavourable to it being the CH_4 conversion at 823 K. By contrast, specific activity and CH_4 conversion at lower temperature (623 K) are neatly unfavourable to $La_{0.9}Sr_{0.1}CoO_3$.

3.2. EPR spectra

The EPR spectra of $La_{0.9}Ce_{0.1}CoO_3$ have been discussed elsewhere [2]. The EPR pattern of $La_{0.9}Sr_{0.1}CoO_3$ at 300 K is composed of two overlapping features characterized by different widths (Fig. 2a). At temperature $T \leq 240$ K the intensity of this pattern decreases, while a new one adds, centred at zero magnetic field value and with opposite phase (Fig. 2b), accompanied by a dramatic increase of the EPR cavity Q-factor. At even lower temperature the zero-field spectrum

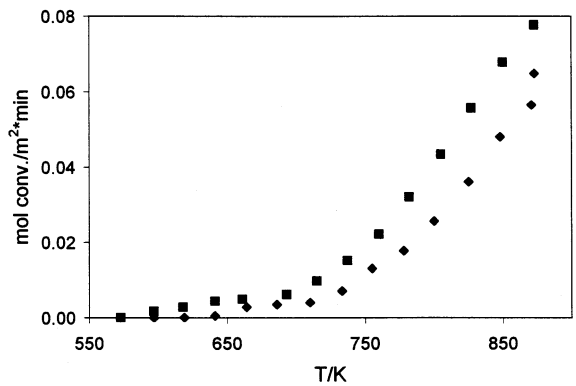

Fig. 1. Specific catalytic activity of $La_{0.9}M_{0.1}CoO_3$. M = (◆) Sr; (■) Ce.

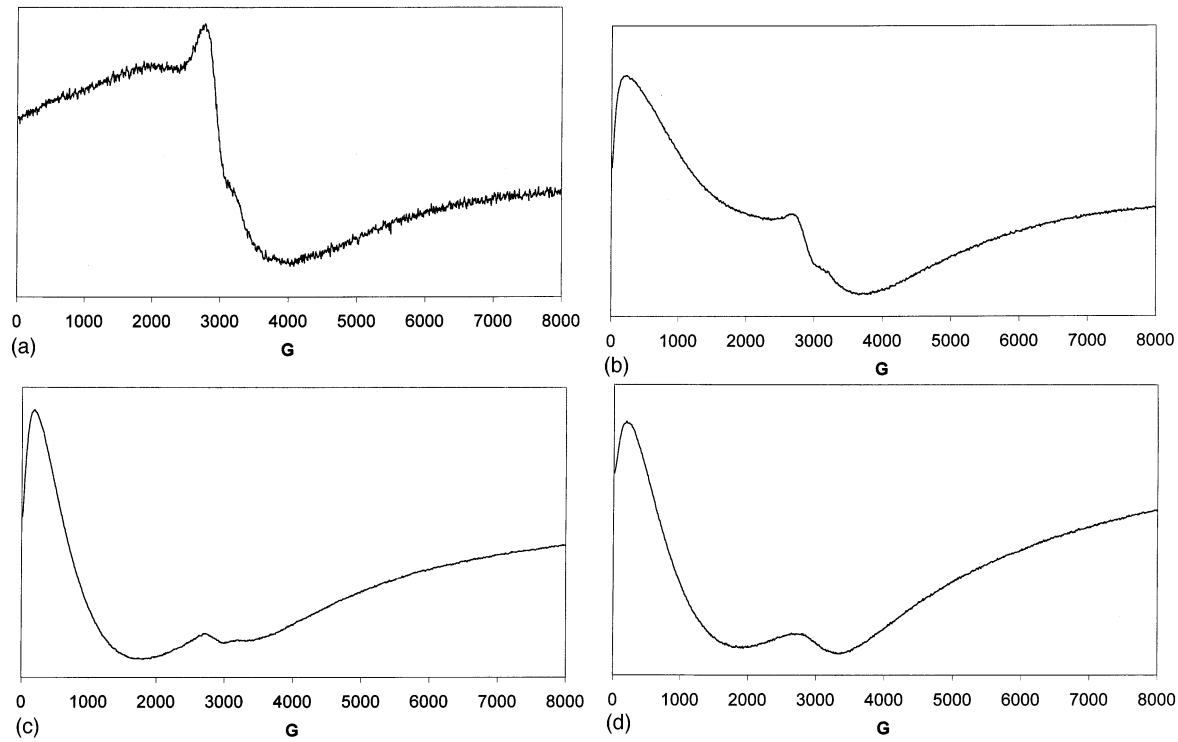

Fig. 2. EPR spectrum of $La_{0.9}Sr_{0.1}CoO_3$ sample, before use as catalyst. Detection temperature: (a) 300 K; (b) 240 K; (c) 210 K; (d) 100 K.

narrows and becomes more intense, at the expenses of the intensity of the $g \cong 2$ one (Fig. 2c). The opposite behaviour is observed only at the lowest examined temperature (100 K), at which the $g \cong 2$ spectrum also changes shape becoming more symmetric (Fig. 2d). After catalytic use for flameless methane combustion, an EPR spectrum at 300 K similar to the broader feature of Fig. 2a is still obtained. By contrast, the narrower line of Fig. 2a is no more noticed (Fig. 3a). At $T \leq 245$ K (5° lower than for fresh sample) the zero-field line appears also with the sample used for the catalytic reaction, narrowing and becoming more intense at lower temperature (Fig. 3b and c) as with the fresh sample. At last, at 100 K the zero-field line becomes a bit broader and less intense also in this case, while the $g \cong 2$ changes shape, acquiring a symmetric (probably Gaussian) shape. Finally, we performed an hysteresis experiment at 125 K both with fresh sample (Fig. 4A) and after catalytic reaction (Fig. 4B). In both the cases the 'up' track (obtained at increasing magnetic field) appeared at higher field than the 'down' one.

4. Discussion

The above mentioned catalytic activity results (Table 1) indicate that the Sr-containing sample is a worse catalyst with respect to the Ce-containing one. This difference in performance is accentuated at lower temperatures, suggesting the presence of a low temperature enhanced phenomenon able to inhibit oxygen exchange with $La_{0.9}Sr_{0.1}CoO_3$. This is in agreement with Temperature Programmed Desorption data reported [1] for samples similar to the ones here examined and showing two peaks at nearly 523 and 873 K, attributed to *suprafacial* and to *intrafacial* oxygen extraction, respectively. In fact, the former peak was by far less evident with Sr-doped than with Ce-doped catalysts. To investigate any temperature-dependent phenom-

ena in $La_{0.9}Sr_{0.1}CoO_3$ oxides, EPR spectra were collected at many different temperatures. No significant change was noticed in these spectra at $T > 300$ K. At these temperatures, the two overlapping patterns of Fig. 2a can be attributed to some paramagnetic oxygen-based species (the narrower with $g \cong 2.3$) and to a species involving cobalt, respectively. The former attribution is suggested by the disappearance of the line after the sample reduction occurring during the catalytic methane oxidation (Fig. 3a). The broad EPR spectrum of Fig. 3a is similar to that reported [2] with $La_{0.9}Ce_{0.1}CoO_3$ and attributed to Co^{3+}/O_2^- pairs (see fitting parameters in the Fig. 3 caption).

The broad and intense absorption feature close to zero field values observed at lower temperatures (Fig. 2b–d and Fig. 3b–d) is rather similar to the ones reported in literature [3–6] with many high temperature super conductors (HTSC), exactly at their superconducting transition temperature. Indeed, in those cases the zero-field pattern was characterized by opposite phase with respect to the one due to the paramagnetic ions. Furthermore, that feature was accompanied by a dramatic increase [7] of the EPR cavity Q-factor, as here noticed by us. At a first glance this low-field absorption was attributed [8] to a strong dipolar coupling [9] between two Cu^{2+} ions, overcoming the Zeeman energy. However, other researchers observed [10] that this absorption was 'non resonant', because it was observed at a nearly-zero magnetic field value, which remained identical after changing the microwave frequency from 9 to 2.4 GHz, and because this feature did not change when changing the microwave polarization plane. Therefore, this low-field line was attributed to trapped-flux in the material. This interpretation was criticized later [11]. However it was further supported [7] by the observation that the low-field line was more intense when a significantly larger

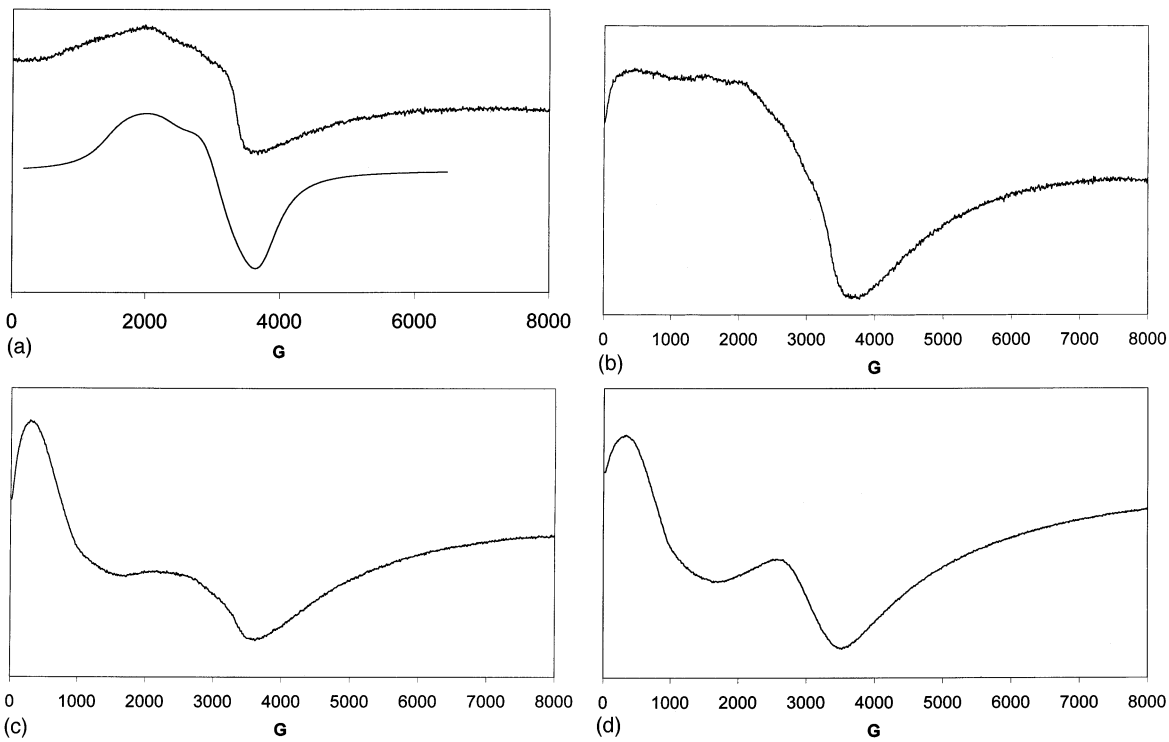

Fig. 3. EPR spectrum of $La_{0.9}Sr_{0.1}CoO_3$ sample, after use as catalyst for flameless combustion of methane. Detection temperature: (a) 300 K; (b) 240 K; (c) 210 K; (d) 100 K. The spectrum obtained at 300 K is compared to its simulation with $A_{xx} = A_{yy} = 100$ G, $A_{zz} = 120$ G, $g_x = g_y = 2$, $g_z = 3.5$, nuclear spin $I = 7/2$, electron spin $S = 1/2$, Lorentzian-shaped components.

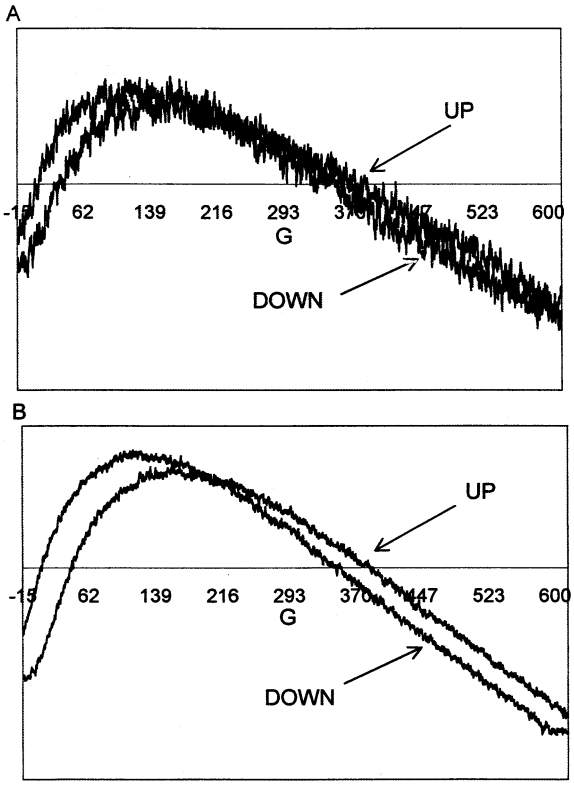

Fig. 4. Hysteresis experiments performed at 125 K with $La_{0.9}Sr_{0.1}CoO_3$ sample: (A) unused; (B) used as catalyst for flameless combustion of methane.

Meissner effect was observed, i.e. in the case in which the magnetic field was more deeply expelled from the sample, below its transition temperature to the superconducting state. Anyway, the origin of this low-field signal remained unclear as long as EPR studies were limited to powdered samples. At last, YBa_2CuO_7 single crystals became available, and a series of very sharp lines was observed [12] with them, 0.212 G split to each other when the magnetic field was directed as the [110] crystal axis. Furthermore, these features behaved quite unexpectedly with crystal rotation. Indeed they moved in such a way that the magnetic field component along the [110] direction remained constant. These phenomena were no more interpretable in the framework of the usual EPR theory only. Indeed, the involvement [12,13] of *Josephson effects* was also invoked. This means that in these materials *weak superconductivity* would occur, due to the presence of superconducting regions separated by insulating layers 1–2 nm thick only, due to non-superconducting grain boundaries or internal grain defects. Then, 'superconducting' electrons could pass through these barriers, by 'tunnel' effect, generating an electron current also in the absence of any electric field (*Stationary Josephson Effect*). Then, when this electric current is intense enough, a difference ΔV of electric potential arises across the insulating layer, generating an alternating current with frequency $v = 2e\Delta V/h$, where e is the electron charge and h the Planck's constant (*non stationary Josephson effect*, NSJE). These *Josephson currents* generate harmonic oscillations of the magnetic flux, representable as a *flux-hopping process* [14]. If the magnetic flux is represented as *fluxon* quasiparticles, then the NSJE can be represented as the absorption of a fluxon inducing a further repulsion among the fluxons already present in the region limited by the insulating layers, and hence inducing also the absorption of a microwave quantum. The last would be at the origin of the nearly-zero-field features observed in those EPR pattern, named low field microwave absorption (LFMA).

At a first glance, LFMA detection seemed a very safe and sensitive procedure [6,15] to test superconductivity of ceramic samples. However, below 260 K LFMA was observed also in a case [16] in which the sample (Gd_2CuO_4) was not a HTSC. The only difference observed between HTSC and this non superconducting sample was that with HTSC the signal appeared at lower fields during external field increasing, than during its decreasing, at the opposite with the case of the non superconducting Gd_2CuO_4 sample. This suggested trapping of magnetic flux lines in a direction opposite to that of the applied field in the case of HTSC, at difference with non-superconducting samples. Therefore, the hysteresis loop of LFMA in a microwave cycle would be proportional to AC susceptibility at microwave frequencies.

Coming to the nature of the physical system undergoing microwave AC magnetization with $La_{0.9}Sr_{0.1}CoO_3$, this must be formed by spin glass, as indicated [16] in the analogous case of

Gd_2CuO_4. A model has been also proposed [17] in which spin glass forms on doping the system with holes, and inducing an attractive interaction between them. According to that model, the hole on oxygen mediates a ferromagnetic coupling between transition metal spins which, otherwise, would couple antiferromagnetically. These two competing magnetic interactions would result in frustration leading to spin glass formation. In the present case, holes are introduced in the lattice when Sr substitutes for La, through the reaction:

$$Sr^{2+}\ O^{2-} \rightarrow Sr'_{La} + O''_i + V^{\cdot\cdot}_o + h^{\cdot} \quad (1)$$

Here, the apex indicates the equivalence of introducing a negative charge and the dot indicates the equivalence of introducing a positive charge into the lattice. Therefore, the sum of apices must equal the sum of dots. In particular, in reaction (1) Sr'_{La} is a defect formed by substituting Sr^{2+} for La^{3+}, $V^{\cdot\cdot}_o$ is an oxygen vacancy and $h^{\bullet}$ is an electron hole such as a high-oxidation-number cobalt paramagnetic ion. As for O''_i, this is an interstitial O_i^{2-} ion in the bulk, while on the surface of internal pores the formation of the paramagnetic O^-_{ads} ions is energetically favoured [18,19].

Furthermore, it has been reported [18–21] that only about a half of O_i^{2-} ions can occupy the $V^{\cdot\cdot}_o$ vacancies in the bulk, forming reticular oxygen O^x_o and leading to:

$$2(Sr^{2+}\ O^{2-}) \rightarrow 2Sr'_{La} + O''_i + O^x_o + V^{\cdot\cdot}_o + 2h^{\cdot} \quad (2)$$

The catalytic oxidation of methane at higher temperatures follows an intrafacial mechanism requiring the presence of O^x_o only. Therefore, after catalytic reaction, O_i^{2-} (or O^-_{ads} on the surface), as well as $h^{\cdot}$, are present in the catalyst. The electrostatic repulsion among particles having charge of the same sign is weakened by the attraction between particles with charge of opposite sign, so that the (competitive) magnetic attraction among all the paramagnetic particles present in the sample (O^-_{ads} and $h^{\cdot}$) can overcome the electrostatic interaction among them, leading to frustration as required [16,17] for spin glass formation. In this case, at enough low temperature the spin glass forms, involving $h^{\cdot}$ (i.e. paramagnetic high-oxidised cobalt ions) as well as O^-_{ads} located on the sample surface. With both fresh and used samples, the formation of LFMA is accompanied by an intensity decrease of the $g \cong 2$ EPR features due to oxygen-based species (with the fresh sample) and to Co^{3+}/O_2^-. This further confirms that both oxygen-based paramagnetic species and cobalt paramagnetic ions are involved in the spin glass formation. At last the nearly symmetric curve fitting the lowest temperature patterns of Fig. 2d and Fig. 3d indicates that ordered structures form at such temperatures, like those already reported [2] for $La_{1-x}Ce_xCoO_3$ samples at temperature lower than 240 K. The fact that these ordered structures are observed at temperatures by far lower with Sr^{2+} than with Ce^{4+} doping [2] can be attributed to the different distortion introduced in the lattice by the two ions, due to their different radius.

In principle, spin glass could be observed also with fresh samples in which Ce^{4+} substitutes for La^{3+}, following the reaction:

$$Ce^{4+}O_2^{2-} \rightarrow Ce^{\cdot}_{La} + 2O''_i + V'_o{}' + h^{\cdot} \quad (3)$$

However no LFMA has been observed by us [2] with these samples, though they were prepared by the same procedure followed here for the Sr-containing sample. This could be due to the fact that the number of O''_i ions is twice that of $h^{\cdot}$ holes in Eq. (3) at difference with Eq. (1) in which the ratio is one-to-one. This could alter the above mentioned competing effect of magnetic interactions among different paramagnetic ions. Furthermore, Ce-containing samples are more easily reoxidized [1] than Sr-containing ones. A complete reoxidation of the former, performed after extraction of O^x_o, would lead to:

$$Ce^{4+}O_2^{2-} \rightarrow Ce^{\cdot}_{La} + O^-_{ads} + O^x_o \quad (4)$$

in which one of the two competing paramagnetic ions, $h^{\cdot}$, is not present anymore.

The lower activity of the Sr-doped sample could then be ascribed to the formation of spin glass involving both paramagnetic Co ions and O^-_{ads} ions. The interaction among these species prevents the cobalt ions to host further oxygen ions, so lowering their availability for the catalytic oxidation reaction.

5. Conclusions

Low temperature EPR spectra of $La_{0.9}Sr_{0.1}CoO_3$ reveal a LFMA pattern due to the formation of spin glass. This involves both oxygen-based species, such as O^-_{ads}, and paramagnetic high-oxidation-number cobalt ions, like Co^{3+} or Co^{4+}, equivalent to electron holes $h^{\bullet}$. Spin glass formation could explain the low ability of this oxide to exchange oxygen and, therefore, its lower catalytic activity with respect to identical samples doped with Ce instead of Sr, in which spin glass is not observed.

Acknowledgements

We are indebted to M. Savoldi and A. D'Ambrosio for collecting EPR spectra and for technical support.

References

[1] D. Ferri, L. Forni, Appl. Catal. B: Environ. 16 (1998) 119.
[2] C. Oliva, L. Forni, A. D'Ambrosio, A. Stepanov, Z. Kagramanov, A.V. Vishniakov et al., work in progress.
[3] K.W. Blazey, K.A. Mueller, J.G. Bednorz, W. Berlinger, G. Amoretti, E. Buluggiu, et al., Phys. Rev. B 36 (1987) 7241.
[4] B.F. Kim, J. Bohandy, K. Moorjani, F.J. Adrian, J. Appl. Phys. 63 (1988) 2029.
[5] R. Jones, R. Janes, R. Armstrong, K.K. Singh, P.P. Edwards, D.J. Keeble, et al., J.C.S. Faraday Trans. 86 (1990) 683.
[6] N. Guskos, V. Likodimos, J. Kuriata, M. Calamiotou, M. Wabia, S.M. Paraskevas, et al., Phys. Stat. Sol. (b) 180 (1993) 491.
[7] C. Rettori, D. Davidov, I. Belaish, I. Felner, Phys. Rev. B. 36 (1987) 4028.
[8] M.D. Sastry, A.G.I. Dalvi, Y. Balu, R.M. Kadan, J.V. Yakhmi, R.M. Iyer, Nature 330 (1987) 49.
[9] E. Wasserman, L.C. Snyder, W.C. Yager, J. Chem. Phys. 41 (1964) 1763.
[10] T.S. Lin, L.G. Sobotka, W. Francisz, Nature 333 (1988) 21.
[11] A.R. Harutyunyan, L.S. Grigoryian, M. Baran, S. Piechota, Phys. Lett. A 133 (1988) 339.
[12] K.W. Blazey, A.M. Portis, K.A. Mueller, F.H. Holtzberg, Europhys. Lett. 6 (1988) 457.
[13] K.W. Blazey, F.H. Holtzberg, IBM J. Res. Devel. 33 (1989) 324.
[14] K.N. Shrivastava, Solid State Commun. 68 (1988) 259.
[15] B. Czyzak, J. Stankowski, Phys. Stat. Sol. b. 166 (1991) 219.
[16] M.D. Sastry, K.S. Ajayakumar, R.M. Kadam, G.M. Phatak, R.M. Iyer, Phys. C 170 (1990) 41.
[17] A. Aharony, R.J. Birgenau, A. Coniglio, M.A. Castner, H.E. Stanley, Phys. Rev. Lett. 60 (1988) 1330.
[18] P.J. Gellings, H.J.M. Bouwmeester, Catal. Today 12 (1992) 1.
[19] A. Bielanski, J. Haber, Catal. Rev. Sci. Eng. 19 (1979) 1.
[20] H.M. Zhang, et al., J. Catal. 121 (1990) 432.
[21] Y. Teraoka et al., Chem. Lett. (1984) 893.